Available online at www.sciencedirect.com

ScienceDirect

Publishing Services by Elsevier

International Journal of Naval Architecture and Ocean Engineering 8 (2016) 615–630
http://www.journals.elsevier.com/international-journal-of-naval-architecture-and-ocean-engineering/

A unified solution for vibration analysis of plates with general structural stress distributions

Nian Yang [a,b], Lu-Yun Chen [a,b], Hong Yi [a,b,*], Yong Liu [c]

[a] State Key Laboratory of Ocean Engineering, Shanghai Jiao Tong University, Shanghai, China
[b] The Collaborative Innovation Center for Advanced Ship and Deep-Sea Exploration, Shanghai, China
[c] Ship Scientific Research Center of China, Shanghai Branch, Shanghai, China

Received 6 March 2016; revised 22 May 2016; accepted 30 May 2016
Available online 7 October 2016

Abstract

Complex stress distributions often exist in ocean engineering structures. This stress influences structural vibrations. Finite Element Methods exhibit some shortcomings for solving non-uniform stress problems, such as an unclear physical interpretation, complicated operation, and large number of computations. Analytical methods research considers mainly uniform stress problems, and often, their methods cannot be applied in practical marine structures with non-uniform stress. In this paper, an analytical method is proposed to solve the vibration of plates with general stress distributions. Non-uniform stress is expressed as a special series, and the stress influence is inserted into a vibration equation that is solved through decoupling to obtain an analytical solution. This method has been verified using numerical examples and can be used in arbitrary stress distribution cases. This method requires fewer computations and it provides a clearer physical interpretation, so it has advantages in some qualitative research.

Keywords: Structural stress; Plate structure; Vibration; Analytical method

1. Introduction

The complexity and special working environment of some practical ocean engineering structures means that often, stress exists in the structure prior to it being subjected to a work load. These stresses include artificial stresses, such as prestress in structural connections; stress caused by manufacturing, such as welding residual and assembly stresses; and stress caused by complex and special working environments, such as submarine shell stresses caused by hydrostatic pressure. It is worth noting that these kinds of stresses could change structural performance.

A large amount of research effort has been devoted to studying the influence of stress on structural strength and fatigue (Dong, 2001; Gannon, 2012; Khan, 2011; Niemi, 1995; Paik, 2012). As we know, the structural vibration is always a research hotspot (Cho, 2016; Senjanović, 2015, 2016). However, in comparison, the influence of stress on vibration is often ignored and limited related research exists in this area. Doong (1987) applied high-order shear deformation theory to derive the initial stress thick plate vibration control equation, and compared results with reference data (Brunelle and Robertson, 1976). Fuller and Fahy (1982) considered pressure caused by fluid filling a cylinder and derived its free vibration equation. Liu and Zhang used the wave propagation method to study the effect of hydrostatic pressure fields on

* Corresponding author. The Collaborative Innovation Center for Advanced Ship and Deep-Sea Exploration, Shanghai, China.
E-mail address: 416272953@qq.com (H. Yi).
Peer review under responsibility of Society of Naval Architects of Korea.

http://dx.doi.org/10.1016/j.ijnaoe.2016.05.013

vibration characteristics (Liu, 2010, 2011; Zhang, 2001, 2002). However, they focused mainly on uniform distributed stress. The influence of stress concentration around holes on vibration has also been studied (Yahnioglu, 2007). Gao (2002, 2014) compared experimentally a plate with and without welding stress. Although their research focused on non-uniform distributed stress, it is limited to specified stress-distribution types and cannot be applied to other distributions. Non-uniform stress distributions are often encountered in ocean engineering structures and these distributions vary in different working environments. The former methods cannot be used to solve this practical stress problem, and a method is required that can solve structural vibrations with general stress distributions.

Although the Finite Element Method (FEM) can be used to investigate structural dynamics with non-uniform stress distributions (Chen et al., 2014), it cannot explain the essential relationship between structural stress and vibration. Complicated operations are required to exert a non-uniform stress distribution and reruns are required when the stress distribution changes. FEM requires high modelling costs, especially for large-scale structures. So, it is inconvenient to conduct research on the stress-caused influence on vibration by FEM. Therefore, it is necessary to develop alternative analytical methods.

This work aims to provide a unified and efficient solution for vibration analysis of structures with general stress distributions. Plate structures are discussed and an analytical method is proposed to solve the vibration problem of non-uniform stressed plates. Using the proposed method, structural stress, regardless of its distribution and value, is expressed as a special series that can express almost all of the stress distributions and achieve partial decoupling among structural modes in the final vibration equation. The analytical solution is obtained by solving this decoupling equation. Finally, this method is verified using numerical examples. The analytical solution can be applied to a structure with arbitrary distributed stress, so it has a wider range of applications than previous analytical methods. It also requires less computation and provides a clearer physical interpretation than FEM, so it is more suited for qualitative research on the relationship between stress and vibration. The proposed method can be applied in the vibration analysis of ships and offshore structures with a non-uniform distributed stress, such as submarine welding stresses, which are distributed only near the joints; risers' varying stresses that are caused by hydrostatic pressure at different water depths; and varying seabed pipeline stresses that are caused by in-pipe fluid with different fluid velocities and temperatures.

Structural stress distributions can be obtained by using some mature methods according to different stress factors, for example, the welding stress (Li, 2010; Radaj, 2012), the hydrostatic pressure-induced stress (Cao, 1989; Liu, 2009), and the in-pipe fluid-induced stress (Bokaian, 2004; Zhang, 2001). Once the stress distribution has been determined, structural vibration with a specific distributed stress can be obtained rapidly using the presented method. This stress-considering vibration result is closer to the reality. By comparing the non-stressed structure's vibration, the level and feature of the stress influence on vibration can be analysed. Based on the vibration results and stress influences, further steps can be taken to resist vibration.

The proposed method also has application in many other engineering applications, such as vibration optimization and damage identification. In future, it may be possible to combine the presented method with innovative materials, such as Functionally Graded Materials (FGMs) (Belabed, 2014; Bellifa, 2016; Bennoun, 2016; Bouderba, 2013; Bourada, 2015; Hamidi, 2015; Hebali, 2014; Mahi, 2015; Meziane, 2014; Tounsi, 2013; Ait Yahia et al., 2015; Zidi, 2014) FGMs are heterogeneous materials in which the material properties are varied continuously from point to point. At each interface, the material is chosen according to specific applications and environmental loadings. Nowadays, FGM is being used increasingly in engineering.

The remainder of this paper is organised as follows: Section 2 builds the vibration equation of the structure with general stress distributions. Section 3 presents the solution procedures of the equation derived in Section 2. In Section 4, some numerical examples are used to verify this method. Section 5 presents the conclusions.

2. Theoretical formulations

2.1. Description of the model

In most previous methods, the stress value is seen as an invariant because it considers mainly the uniform stress distribution case (Fuller and Fahy, 1982; Liu et al., 2010, 2011; Zhang et al., 2001a,b, 2002), and these invariants are substituted into the vibration equation to obtain the vibration equation of uniform stressed structures. However, the aim of this study is a plate with arbitrary stress distributions as shown in Fig. 1, and the stress value varies with different locations. So, the basic vibration equation of structure with a non-uniform stress needs to be derived. In Fig. 1, h is the thickness; a is the plate length; b is the plate width; the x axis represents the length direction; the y axis represents the width direction; and u, v, and w are the neutral plane displacements in the x, y, and z directions, respectively. Stresses can be divided into a normal stress σ_x^r and σ_y^r and a shear stress τ_{xy}^r, and their stress amplitudes are functions of x and y.

Before the derivation, the following assumptions are made:

(1) Fluid–Structural Interaction is not considered in this paper.
(2) Structural stresses and stresses caused by vibration satisfy the linear superposition.
(3) The vibration satisfies the small elastic deformation condition.
(4) The stress is distributed uniformly in the thickness direction.
(5) Stress relief is not considered in this paper.

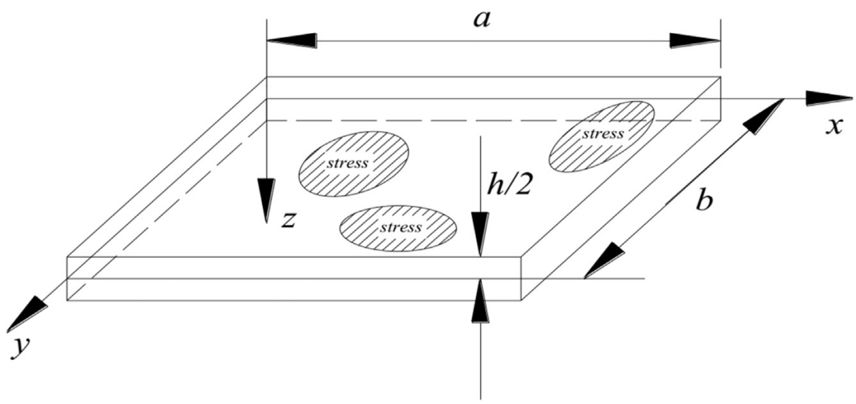

Fig. 1. Plate with general structural stress distribution.

2.2. Coupling force between vibration and stress

In an element body from the plate, the length and width directions are dx and dy, respectively, and the z axis represents the normal direction of this element body. When the plate is static, the force diagram of an element with structural stress is shown in Fig. 2.

In Fig. 2, N_x^r and N_y^r represent unit length section tensile forces in the x and y directions, respectively, and N_{xy}^r and N_{yx}^r represent unit length shear forces in the x and y directions, respectively. According to the definition of stress, these can be expressed as:

$$\begin{cases} N_x^r = \sigma_x^r S_x = \sigma_x^r h \\ N_y^r = \sigma_y^r S_y = \sigma_y^r h \\ N_{xy}^r = N_{yx}^r = \tau_{xy}^r S_{xy} = \tau_{xy}^r h \end{cases}. \tag{1}$$

When the plate is vibrating, the forces and moments of the element body can be divided into two parts: Part 1 consists of the forces and moments caused by vibration deformations, as shown in Fig. 3; Part 2 consists of the coupling forces and moments caused by structural stress and vibrational displacements. The former part can be expressed by classic thin-plate theory (Cao, 1989). The latter part is derived below.

It is assumed that the structural stress remains unchanged during vibration. So when the neutral plane is of unit length, the unit lengths in sections OA and OC (in Fig. 4) with distance z from the neutral plane are:

$$\begin{cases} l_{\mathrm{OC}}^z = 1 + \varepsilon_x \\ l_{\mathrm{OA}}^z = 1 + \varepsilon_y \end{cases}. \tag{2}$$

Hence, the unit length section areas of OA and OC become:

$$\begin{cases} S_x = \int_{-\frac{h}{2}}^{\frac{h}{2}} l_{\mathrm{OC}}^z dz = h \\ S_y = \int_{-\frac{h}{2}}^{\frac{h}{2}} l_{\mathrm{OA}}^z dz = h \end{cases}. \tag{3}$$

From Eq. (3), the unit length section areas of OA and OC do not change with vibration, and so neither does N_x^r.

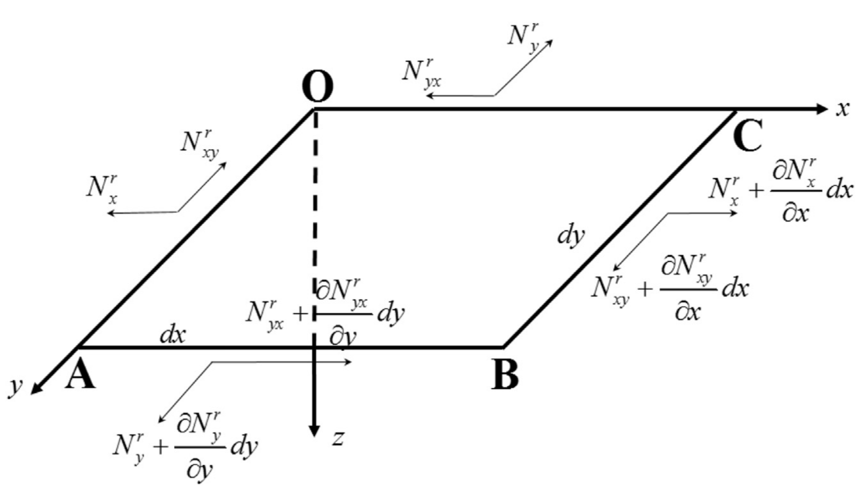

Fig. 2. Section force caused by structural stress.

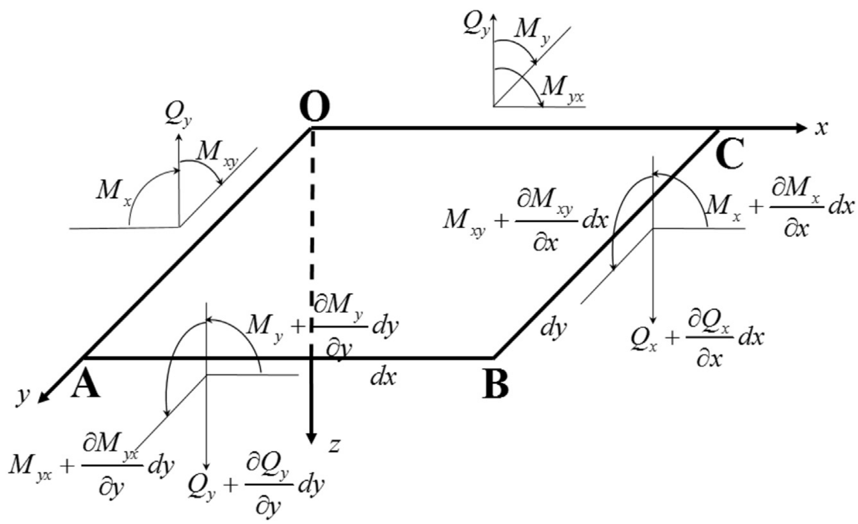

Fig. 3. Section force and moment caused by vibration.

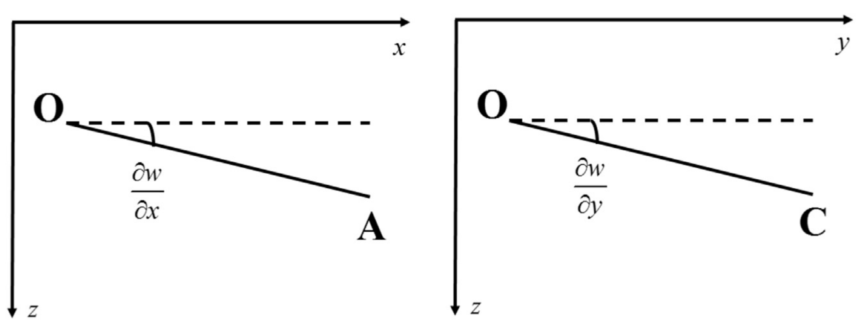

Fig. 4. Element angle.

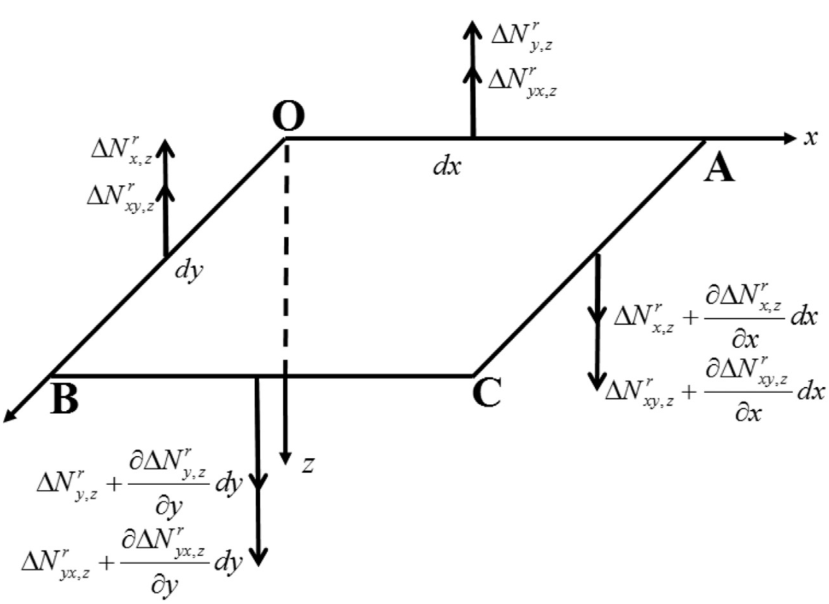

Fig. 5. Element body coupling forces.

However, because of the displacement w, N_x^r is no longer parallel to axis x, and an angle exists around the y axis, $\frac{\partial w}{\partial x}$ as shown in Fig. 5. Hence, N_x^r has a new component $N_{x,z}^r$ in the z direction, which can be expressed as:

$$N_{x,z}^r = \sigma_x^r h \frac{\partial w}{\partial x}. \tag{4}$$

Eq. (4) shows that the new component $N_{x,z}^r$ is related to the stress and vibrational displacement. It is termed the *coupling force* between the stress and vibration and $N_{x,z}^r$ is denoted as $\Delta N_{x,z}^r$ in the following. The new components of N_y^r, N_{xy}^r, andN_{yx}^r in the z direction can be obtained in a similar way:

$$\begin{cases} \Delta N_{y,z}^r = \sigma_x^r h \dfrac{\partial w}{\partial y} \\ \Delta N_{xy,z}^r = \tau_{xy}^r h \dfrac{\partial w}{\partial y}. \\ \Delta N_{yx,z}^r = \tau_{yx}^r h \dfrac{\partial w}{\partial x} \end{cases} \tag{5}$$

Based on the Kirchhoff thin-plate theory, the stress remains unchanged in the thickness direction. So the coupling moments and torques caused by structural stresses in this paper should not be considered.

2.3. Vibration equation of structure with general stress distributions

From the derivation above, it is clear that structural stress and vibrational displacement produce some new coupling forces during vibration, and these coupling forces could affect the force equilibrium equations. So the vibration equation would change and new force and moment equilibrium equations need to be derived.

According to the derivation above, no new coupling forces are generated in the x and y directions, so the force equilibrium equations in the x and y directions are still satisfied. Only the new force equilibrium equation in the z direction and the moment equilibrium equations need to be built.

(1) new force equilibrium equation in z direction

In stressed structures, besides vibration-induced shear forces Q_x and Q_y (in Fig. 3), the new coupling forces $\Delta N_{x,z}^r$, $\Delta N_{y,z}^r$, $\Delta N_{xy,z}^r$, and $\Delta N_{yx,z}^r$ (in Fig. 5) are generated. So, the force equilibrium equation in direction z can be expressed as:

$$\begin{aligned} &\frac{\partial Q_x}{\partial x} dxdy + \frac{\partial Q_y}{\partial y} dydx + \frac{\partial \Delta N_{x,z}^r}{\partial x} dxdy + \frac{\partial \Delta N_{y,z}^r}{\partial y} dydx \\ &+ \frac{\partial \Delta N_{xy,z}^r}{\partial x} dxdy + \frac{\partial \Delta N_{yx,z}^r}{\partial y} dydx = \rho h \frac{\partial^2 w}{\partial t^2} dxdy \end{aligned} \tag{6}$$

(2) moment equilibrium equations

Because new coupling moments are not considered in this paper, and based on the Kirchhoff thin-plate theory, the moment equilibrium equations in the x and y directions, respectively, are:

$$Q_y dxdy + \frac{\partial M_{xy}}{\partial x} dxdy + \frac{\partial M_y}{\partial y} dydx = 0; \tag{7}$$

$$Q_x dydx + \frac{\partial M_{yx}}{\partial y} dydx + \frac{\partial M_x}{\partial x} dxdy = 0. \tag{8}$$

Substitution of Eqs. (7) and (8) into Eq. (6) yields:

$$\begin{aligned} \frac{\partial^2 M_x}{\partial x^2} + 2\frac{\partial^2 M_{xy}}{\partial x \partial y} + \frac{\partial^2 M_y}{\partial y^2} - \Bigg[&\frac{\partial \Delta N_{x,z}^r}{\partial x} + \frac{\partial \Delta N_{y,z}^r}{\partial y} \\ &+ \frac{\partial \Delta N_{xy,z}^r}{\partial x} + \frac{\partial \Delta N_{yx,z}^r}{\partial y} \Bigg] = -\rho h \frac{\partial^2 w}{\partial t^2}. \end{aligned} \tag{9}$$

Substitution of Eqs. (4) and (5) into Eq. (9) yields the stressed plate vibration equation:

$$L(w) - C\left(w, \sigma_x^r, \sigma_y^r, \tau_{xy}^r\right) = -\frac{\rho h}{D} \frac{\partial^2 w}{\partial t^2}, \tag{10}$$

where $L(w) = \frac{\partial^4 w}{\partial x^4} + 2\frac{\partial^4 w}{\partial x^2 \partial y^2} + \frac{\partial^4 w}{\partial y^4}$;

$$\begin{aligned} C\left(w, \sigma_x^r, \sigma_y^r, \tau_{xy}^r\right) = \frac{h}{D} \Bigg[&\frac{\partial}{\partial x}\left(\sigma_x^r \frac{\partial w}{\partial x}\right) + \frac{\partial}{\partial y}\left(\sigma_y^r \frac{\partial w}{\partial y}\right) \\ &+ \frac{\partial}{\partial x}\left(\tau_{xy}^r \frac{\partial w}{\partial y}\right) + \frac{\partial}{\partial y}\left(\tau_{xy}^r \frac{\partial w}{\partial x}\right) \Bigg]; \end{aligned}$$

ρ is the structure density, h is the shell thickness, $D = \frac{Eh^3}{12(1-\mu^2)}$ is the bending stiffness, μ is Poisson's ratio, and E is the Young's modulus.

Equation (10) is the vibration equation of a plate with a general stress distribution, and $C(w, \sigma_x^r, \sigma_y^r, \tau_{xy}^r)$ represents coupling between the structural stress and the vibration. Because the values of σ_x^r, σ_y^r, andτ_{xy}^r vary with change in location, the partial derivatives cannot be ignored either.

Former research mainly used this equation to solve the vibration problem of the structure with uniform stress, which means that σ_x^r, σ_y^r, and τ_{xy}^r are constants. They are substituted into Eq. (10) to solve the vibration (Cao, 1989). However, the present research considers the general stress distribution, whose stress amplitude varies with change in location. So, former methods cannot be used here, and a new solution method is required.

3. Solution of the vibration equation

The boundary condition is assumed as simply supported and the displacement can be expressed in the series (He, 2001):

$$w = \sum_{\eta=1}^{M} \sum_{\zeta=1}^{N} W_{\eta\zeta} \sin(\eta \alpha x) \sin(\zeta \beta y) \sin(\omega t), \tag{11}$$

where $W_{\eta\varsigma}$ is the series coefficient, $\alpha = \frac{\pi}{a}$, $\beta = \frac{\pi}{b}$, and a and b are the plate length and width, respectively.

By substituting Eq. (11) into Eq. (10), multiplying both sides of Eq. (10) by $sin(m\alpha x)$ and $sin(n\beta y)$ and using the trigonometric function's orthogonality, the complex stressed plate dynamic equation is derived:

$$\left[(m\alpha)^2+(n\beta)^2\right]^2 W_{mn} - \frac{4}{ab}\int_0^a\int_0^b C\sin(m\alpha x)\sin(n\beta y)dxdy = -\frac{\rho h\omega^2}{D}W_{mn}, \tag{12}$$

Express the C integration term in Eq. (12) as $K=\int_0^a\int_0^b C\sin(m\alpha x)\sin(n\beta y)dxdy$, which represents the effects of structural stress. Because of the appearance of K, the structural modes couple together, and a single structural mode

$$\begin{aligned} K &= \int_0^a\int_0^b C\sin(m\alpha x)\sin(n\beta y)dxdy \\ &= \frac{h}{D}\Bigg[-\sum_{\eta=1}^{M}\sum_{\varsigma=1}^{N}W_{\eta\varsigma}(\eta\alpha)^2\int_0^a\int_0^b\sigma_g^{rx}\cos(g\alpha x)\sin(\eta\alpha x)\sin(\varsigma\beta y)\sin(m\alpha x)\sin(n\beta y)dxdy- \\ &\quad \sum_{\eta=1}^{M}\sum_{\varsigma=1}^{N}W_{\eta\varsigma}(\varsigma\beta)^2\int_0^a\int_0^b\sigma_j^{ry}\cos(j\beta y)\sin(\eta\alpha x)\sin(\varsigma\beta y)\sin(m\alpha x)\sin(n\beta y)dxdy- \\ &\quad \sum_{\eta=1}^{M}\sum_{\varsigma=1}^{N}W_{\eta\varsigma}\eta g\alpha^2\int_0^a\int_0^b\sigma_g^{rx}\sin(g\alpha x)\cos(\eta\alpha x)\sin(\varsigma\beta y)\sin(m\alpha x)\sin(n\beta y)dxdy- \\ &\quad \sum_{\eta=1}^{M}\sum_{\varsigma=1}^{N}W_{\eta\varsigma}\varsigma j\beta^2\int_0^a\int_0^b\sigma_j^{ry}\sin(j\beta y)\sin(\eta\alpha x)\cos(\varsigma\beta y)\sin(m\alpha x)\sin(n\beta y)dxdy\Bigg] \end{aligned} \tag{14}$$

can no longer be computed so that the entire coupling equation has to be solved in order to obtain the coupling modes.

The C integration term in Eq. (12) is expressed as $K=\int_0^a\int_0^b C\sin(m\alpha x)\sin(n\beta y)dxdy$, which represents the effects of structural stress. Because of the appearance of K, the structural modes couple together, and a single structural mode can no longer be computed so that the entire coupling equation has to be solved to obtain the coupling modes.

The processing of stress is important. If stress is distributed uniformly overall, C is invariant, then the structural modes are uncoupled and the equation is easy to solve. In the present case, C is a general expression of location that leads to structural mode coupling. An appropriate stress expression is required that cannot only represent most stress distributions, but also helps achieve structural mode decoupling. In this paper, a trigonometric series was chosen, which can satisfy the above requirements. One-dimensional stress (the stress value varies in only one direction) and two-dimensional stress (the stress value varies in two directions) are considered in this paper.

3.1. One-dimensional stress type

Consider only the normal stress in this paper. If the stress value varies in one direction, then the one-dimensional structural stress can be expressed as:

$$\begin{cases}\sigma_x^r = \sigma_g^{rx}\cos(g\alpha x)\\ \sigma_y^r = \sigma_j^{ry}\cos(j\beta y)\end{cases}, \tag{13}$$

where σ_g^{rx} and σ_j^{ry} are the x- and y-directional stress amplitude components, respectively, and g and j are positive integers. Substituting Eq. (13) into K yields:

According to the product to sum formula:

$$\begin{aligned} &\int_0^a\cos(g\alpha x)\sin(\eta\alpha x)\sin(m\alpha x)dx \\ &= \int_0^a\frac{1}{2}\{\sin[(\eta+g)\alpha x]+\sin[(\eta-g)\alpha x]\}\sin(m\alpha x)dx \\ &= \int_0^a\frac{1}{2}\sin[(\eta+g)\alpha x]\sin(m\alpha x)dx \\ &\quad + \int_0^a\frac{1}{2}\sin[(\eta-g)\alpha x]\sin(m\alpha x)dx; \end{aligned} \tag{15}$$

$$\int_0^a \sin(g\alpha x)\cos(\eta\alpha x)\sin(m\alpha x)dx$$
$$=\frac{1}{2}\int_0^a\{\sin[(\eta+g)\alpha x]-\sin[(\eta-g)\alpha x]\}\sin(m\alpha x)dx$$
$$=\frac{1}{2}\int_0^a \sin[(\eta+g)\alpha x]\sin(m\alpha x)d\varphi \tag{16}$$
$$-\frac{1}{2}\int_0^a \sin[(\eta-g)\alpha x]\sin(m\alpha x)dx.$$

According to the orthogonality of the trigonometric function:

$$\frac{1}{2}\int_0^a \sin[(\eta-g)\alpha x]\sin(m\alpha x)dx=\begin{cases} a/4 & m+g=\eta \\ 0 & m+g\neq\eta \end{cases}; \tag{17}$$

$$\frac{1}{2}\int_0^a \sin[(\eta+g)\alpha x]\sin(m\alpha x)dx=\begin{cases} a/4 & m-g=\eta \\ -a/4 & m-g=-\eta \\ 0 & |m-g|\neq\eta \end{cases}. \tag{18}$$

Using Eqs. (15)–(18), the first and third terms can be simplified into:

$$\sum_{\eta=1}^{M}\sum_{\varsigma=1}^{N} W_{\eta\varsigma}(\eta\alpha)^2\int_0^b\int_0^a \sigma_g^{rx}\cos(g\alpha x)\sin(\eta\alpha x)\sin(\varsigma\beta y)\sin(m\alpha x)\sin(n\beta y)dxdy$$
$$\begin{cases} =\dfrac{abh}{8D}\sigma_g^{rx}\left\{W_{(m-g)n}[(m-g)\alpha]^2+W_{(m+g)n}[(m+g)\alpha]^2\right\} & m>g \\ =\dfrac{abh}{8D}\sigma_g^{rx}\left\{-W_{|m-g|n}[(m-g)\alpha]^2+W_{(m+g)n}[(m+g)\alpha]^2\right\} & m<g \end{cases} \tag{19}$$

$$\sum_{m=1}^{M}\sum_{n=1}^{N} W_{\eta\varsigma}\eta g\alpha^2\int_0^b\int_0^a \sigma_g^{rx}\sin(g\alpha x)\cos(\eta\alpha x)\sin(\varsigma\beta y)\sin(m\alpha x)\sin(n\beta y)\,dxdy$$
$$\begin{cases} =\dfrac{abh}{8D}\sigma_g^{rx}\left\{W_{(m-g)n}[(m-g)g]\alpha^2-W_{(m+g)n}[(m+g)g]\alpha^2\right\} & m>g \\ =\dfrac{abh}{8D}\sigma_g^{rx}\left\{-W_{|m-g|n}[(m-g)g]\alpha^2-W_{(m+g)n}[(m+g)g]\alpha^2\right\} & m<g \end{cases} \tag{20}$$

Eqs. (19) and (20) means the coupling occurred among the specified modes only. Each mode is coupled with only a few specific modes, rather than with all the other modes. We can simplify the second and fourth terms in the same way. Therefore, for the final vibration equation, we just need to compute the terms which correspond to the specific coupling modes. What is more, after simplification the calculations do not involve integral operations any more. And the simplification does not involve any approximation. So the decoupling of partial modes can reduce the computation cost dramatically without accuracy loss. Then $M \times N$ equations can be constructed and expressed into a matrix form:

Eqs. (19) and (20) imply that coupling occurred among specified modes only. Each mode is coupled with only a few specific modes, rather than with all the other modes. The second and fourth terms can be simplified in the same way. Therefore, for the final vibration equation, terms that correspond with specific coupling modes need to be computed. Moreover, the calculations no longer involve integral operations after simplification. And the simplification does not involve any approximation. So the decoupling of partial modes can reduce the computation cost significantly without loss in accuracy. $M \times N$ equations can be constructed and expressed in a matrix form:

$$\left(\boldsymbol{\Lambda}+\boldsymbol{R}_{gj}\right)\boldsymbol{X}=0 \tag{21}$$

where $\boldsymbol{X}=\{\boldsymbol{W}_1 \ldots \boldsymbol{W}_{(m-1)\times N+n} \ldots \boldsymbol{W}_{M\times N}\}^T$; $\boldsymbol{\Lambda}$ is a sparse diagonal matrix that represents the non-stress part, and its diagonal elements are $\delta_{(m-1)\times N+n}=[(m\alpha)^4+2(mn\alpha\beta)^2+(n\beta)^4]-\frac{\rho h}{D}\omega^2$ and $\boldsymbol{R}_{gj}$ is a sparse non-diagonal matrix, whose elements are:

when $p=(m-1)\times N+n$ and $q=(|m-g|-1)\times N+n$,

$$R_{pq}=\begin{cases} \dfrac{h}{2D}\sigma_g^{rx}(m-g)m\alpha^2 & m>g \\ -\dfrac{h}{2D}\sigma_g^{rx}(m-g)m\alpha^2 & m<g \end{cases}; \tag{22}$$

when $p = (m-1) \times N + n$ and $q = (m+g-1) \times N + n$,

$$R_{pq} = \frac{h}{2D}\sigma_g^{rx}(m+g)m\alpha^2; \tag{23}$$

when $p = (m-1) \times N + n$ and $q = (m-1) \times N + |n-j|$,

$$R_{pq} = \begin{cases} \dfrac{h}{2D}\sigma_j^{ry}(n-j)n\beta^2 & n > j \\ -\dfrac{h}{2D}\sigma_j^{ry}(n-j)n\beta^2 & n < j \end{cases}; \tag{24}$$

when $p = (m-1) \times N + n$ and $q = (m-1) \times N + n + j$,

$$R_{pq} = \frac{h}{2D}\sigma_j^{ry}(n+j)n\beta^2. \tag{25}$$

When the stress distribution is more complicated, the stress can be expressed in series as:

$$\begin{cases} \sigma_x^r = \sigma_g^{rx}\sum_{g=1}^{G}\cos(g\alpha x) \\ \sigma_y^r = \sigma_j^{ry}\sum_{j=1}^{J}\cos(j\beta y) \end{cases}. \tag{26}$$

Applying the same methods as above, a $M \times N$ matrix equation is established:

$$(\boldsymbol{\Lambda} + \boldsymbol{R})\boldsymbol{X} = 0, \tag{27}$$

where the complex stress-matrix, $\boldsymbol{R}$, can also be expressed as a series:

$$\boldsymbol{R} = \sum_{g=1}^{G}\sum_{j=1}^{J}\boldsymbol{R}_{gj}. \tag{28}$$

3.2. Two-dimensional stress type

If the stress value varies in two directions, the two-dimensional structural stress can be expressed as:

$$\begin{cases} \sigma_x^r = \sigma_{gj}^{rx}\cos(g\alpha x)\cos(j\beta y) \\ \sigma_y^r = \sigma_{gj}^{ry}\cos(g\alpha x)\cos(j\beta y) \end{cases}. \tag{29}$$

σ_g^{rx}, σ_j^{ry}, g, and j in Eq. (29) are the same as in Eq. (13). In this case, σ_g^{rx} and σ_j^{ry} are functions of x and y, so they are called a two-dimensional stress.

By substituting Eq. (29) into K, and taking advantage of Eqs. (15)–(18), and simplifying the first and third terms in K yields:

$$\sum_{\eta=1}^{M}\sum_{\varsigma=1}^{N}W_{\eta\varsigma}(m\alpha)^2\int_0^b\int_0^a \sigma_x^r\sin(\eta\alpha x)\sin(\varsigma\beta y)\sin(m\alpha x)\sin(n\beta y)dxdy$$

$$\begin{cases} = \dfrac{abh}{16D}\sigma_{gj}^{rx}\{W_{(m-g)(n-j)}[(m-g)\alpha]^2 + W_{(m-g)(n+j)}[(m-g)\alpha]^2 + \\ \quad W_{(m+g)(n-j)}[(m-g)\alpha]^2 + W_{(m+g)(n+j)}[(m+g)\alpha]^2\} & m > g \text{ and } n > j \\ = \dfrac{abh}{16D}\sigma_{gj}^{rx}\{-W_{(m-g)|n-j|}[(m-g)\alpha]^2 + W_{(m-g)(n+j)}[(m-g)\alpha]^2 - \\ \quad W_{(m+g)|n-j|}[(m+g)\alpha]^2 + W_{(m+g)(n+j)}[(m+g)\alpha]^2\} & m > g \text{ and } n < j \\ = \dfrac{abh}{16D}\sigma_{gj}^{rx}\{-W_{|m-g|(n-j)}[(m-g)\alpha]^2 - W_{|m-g|(n+j)}[(m-g)\alpha]^2 + \\ \quad W_{(m+g)|n-j|}[(m+g)\alpha]^2 + W_{(m+g)(n+j)}[(m+g)\alpha]^2\} & m < g \text{ and } n > j \\ = \dfrac{abh}{16D}\sigma_{gj}^{rx}\{W_{|m-g||n-j|}[(m-g)\alpha]^2 + W_{|m-g|n+j}[(m-g)\alpha]^2 + \\ \quad W_{(m+g)|n-j|}[(m+g)\alpha]^2 + W_{(m+g)(n+j)}[(m+g)\alpha]^2\} & m < g \text{ and } n < j \end{cases} \tag{30}$$

$$\sum_{\eta=1}^{M}\sum_{\varsigma=1}^{N}W_{mn}(m\alpha)^2\int_0^b\int_0^a\frac{\partial\sigma_x^r}{\partial x}\sin(\eta\alpha x)\sin(\varsigma\beta y)\sin(m\alpha x)\sin(n\beta y)dxdy$$

$$\begin{cases} = -\dfrac{abh}{16D}\sigma_{gj}^{rx}\{W_{(m-g)(n-j)}[(m-g)g]\alpha^2+W_{(m-g)(n+j)}[(m-g)g]\alpha^2- \\ \quad W_{(m+g)(n-j)}[(m+g)g]\alpha^2-W_{(m+g)(n+j)}[(m+g)g]\alpha^2\} & m>g \text{ and } n>j \\ = -\dfrac{abh}{16D}\sigma_{gj}^{rx}\{-W_{(m-g)|n-j|}[(m-g)g]\alpha^2+W_{(m-g)(n+j)}[(m-g)g]\alpha^2+ \\ \quad W_{(m+g)|n-j|}[(m+g)g]\alpha^2-W_{(m+g)(n+j)}[(m+g)g]\alpha^2\} & m>g \text{ and } n<j \\ = -\dfrac{abh}{16D}\sigma_{gj}^{rx}\{-W_{|m-g|(n-j)}[(m-g)g]\alpha^2-W_{|m-g|(n+j)}[(m-g)g]\alpha^2- \\ \quad W_{(m+g)(n-j)}[(m+g)g]\alpha^2-W_{(m+g)(n+j)}[(m+g)g]\alpha^2\} & m<g \text{ and } n>j \\ = -\dfrac{abh}{16D}\sigma_{gj}^{rx}\{W_{|m-g||n-j|}[(m-g)g]\alpha^2+W_{|m-g|(n+j)}[(m-g)g]\alpha^2- \\ \quad W_{(m+g)|n-j|}[(m+g)g]\alpha^2-W_{(m+g)(n+j)}[(m+g)g]\alpha^2\} & m<g \text{ and } n<j \end{cases} \tag{31}$$

Eqs. (30) and (31) mean that the coupling occurred among specified modes only. Each mode is coupled with only a few specific modes, rather than with all the other modes. Similarly, the second and fourth terms in K can be simplified. Then $M \times N$ equations can be constructed and expressed in matrix form:

$$(\boldsymbol{\Lambda}+\boldsymbol{R}_{gj})\boldsymbol{X}=0. \tag{32}$$

$\boldsymbol{\Lambda}$ and $\boldsymbol{X}$ in Eq. (32) are the same as those in Eq. (21) and $\boldsymbol{R}_{gj}$ is a sparse non-diagonal matrix, whose elements are: when $p=(m-1)\times N+n$ and $q=(|m-g|-1)\times N+|n-j|$,

$$R_{pq}^{gj}=\begin{cases}\dfrac{h}{4D}\left[\sigma_{gj}^{rx}(m-g)m\alpha^2+\sigma_{gj}^{ry}(n-j)n\beta^2\right] & m>g \text{ and } n>j\\ \dfrac{h}{4D}\left[\sigma_{gj}^{rx}(m-g)m\alpha^2-\sigma_{gj}^{ry}(n-j)n\beta^2\right] & m>g \text{ and } n<j\\ \dfrac{h}{4D}\left[-\sigma_{gj}^{rx}(m-g)m\alpha^2+\sigma_{gj}^{ry}(n-j)n\beta^2\right] & m<g \text{ and } n>j\\ \dfrac{h}{4D}\left[\sigma_{gj}^{rx}(m-g)m\alpha^2+\sigma_{gj}^{ry}(n-j)n\beta^2\right] & m<g \text{ and } n<j\end{cases}; \tag{33}$$

when $p=(m-1)\times N+n$ and $q=(|m-g|-1)\times N+n+j$,

$$R_{pq}^{gj}=\begin{cases}\dfrac{h}{4D}\left[\sigma_{gj}^{rx}(m-g)m\alpha^2+\sigma_{gj}^{ry}(n+j)n\beta^2\right] & m>g\\ \dfrac{h}{4D}\left[-\sigma_{gj}^{rx}(m-g)m\alpha^2+\sigma_{gj}^{ry}(n+j)n\beta^2\right] & m<g\end{cases}; \tag{34}$$

when $p=(m-1)\times N+n$ and $q=(m+g-1)\times N+|n-j|$,

$$R_{pq}^{gj}=\begin{cases}\dfrac{h}{4D}\left[\sigma_{gj}^{rx}(m+g)m\alpha^2+\sigma_{gi}^{ry}(n-j)n\beta^2\right] & n>j\\ \dfrac{h}{4D}\left[\sigma_{gj}^{rx}(m+g)m\alpha^2-\sigma_{gj}^{ry}(n-j)n\beta^2\right] & n<j\end{cases}; \tag{35}$$

when $p=(m-1)\times N+n$ and $q=(m+g-1)\times N+n+j$,

$$R_{pq}^{gj}=\frac{h}{4D}\left[\sigma_{gj}^{rx}(m+g)m\alpha^2+\sigma_{gi}^{ry}(n+j)n\beta^2\right]. \tag{36}$$

When the stress distribution is more complicated, the stress can be expressed in series as:

$$\begin{cases}\sigma_x^r=\sum_{g=1}^{G}\sum_{j=1}^{J}\sigma_{gj}^{rx}\cos(g\alpha x)\cos(j\beta y)\\ \sigma_y^r=\sum_{g=1}^{G}\sum_{j=1}^{J}\sigma_{gj}^{ry}\cos(g\alpha x)\cos(j\beta y)\end{cases}. \tag{37}$$

Applying the same methods as above, a $M \times N$ matrix equation is established:

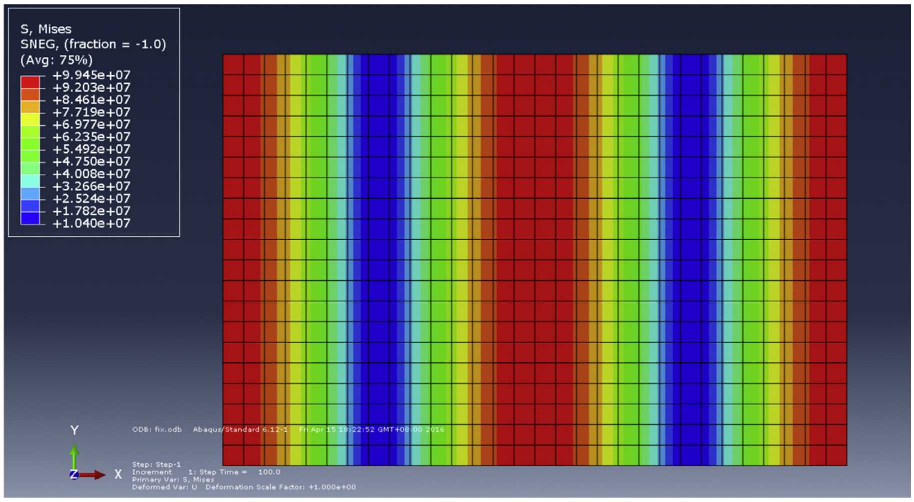

Fig. 6. Stressed plate model.

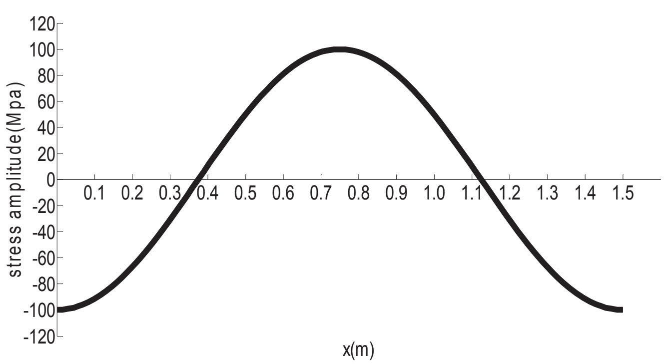

Fig. 7. Structural stress distribution.

$$(\boldsymbol{\Lambda} + \boldsymbol{R})\boldsymbol{X} = 0, \tag{38}$$

where the complex stress-matrix, $\boldsymbol{R}$, can also be expressed as a series:

$$\boldsymbol{R} = \sum_{g=1}^{G} \sum_{j=1}^{J} \boldsymbol{R}_{gj}. \tag{39}$$

Most distributions can be expressed in the form of Eqs. (26) and (37). Hence, the presented method can be applied to deal with the vibration of structure with arbitrary stress distribution.

For free vibration solving, the determinant of Eqs. (27) and (38) should equal zero:

$$|\boldsymbol{\Lambda} + \boldsymbol{R}| = 0. \tag{40}$$

Table 1
Results comparison between the presented method and FEM.

Order	(m,n)	Natural frequency (Hz)								
		Non-stress	With stress	With stress						
			Presented method	FEM						
				0.1 m	0.08 m	0.05 m	0.04 m	0.03 m	0.02 m	0.01 m
1	(1, 1)	35.45	14.86	16.27	15.67	15.17	14.97	14.89	14.77	14.61
2	(2, 1)	68.18	60.96	62.80	62.08	61.40	61.19	61.08	60.95	60.81
3	(1, 2)	109.09	105.00	110.08	107.96	106.24	105.78	105.44	105.16	104.97
4	(3, 1)	122.73	117.69	123.31	121.12	119.04	118.46	118.11	117.80	117.55
5	(2, 2)	141.82	139.70	144.47	142.47	140.81	140.35	140.01	139.71	139.44
6	(3, 2)	196.36	193.87	200.84	198.01	195.44	194.74	194.25	193.81	193.40
7	(4, 1)	199.09	196.03	212.26	205.85	199.80	198.26	197.25	196.43	195.88
8	(1, 3)	231.82	230.09	256.17	244.87	236.04	233.80	232.11	230.83	230.07
9	(2, 3)	264.54	263.84	286.03	277.44	269.24	267.13	265.54	264.31	263.49
10	(4, 2)	272.72	270.64	287.89	279.88	274.08	272.57	271.53	270.66	269.96

Table 2
DOF comparison between the presented method and FEM.

The number of the series used by the presented method	FEM DOF						
	0.1 m	0.08 m	0.05 m	0.04 m	0.03 m	0.02 m	0.01 m
100	612	1055	2712	4384	7764	18,012	73,512

When no stress exists in the structure, i.e., $\boldsymbol{R}=0$, Eq. (40) becomes the classical plate free vibration characteristic equation. Otherwise, the structure modes would couple and change because $\boldsymbol{R}\neq 0$. The arbitrarily stressed structure's natural frequency and mode shape can be obtained by solving Eq. (40).

If the plate is excited by a vertical distributed force f_z, then the forced vibration equation of the stressed plate can be:

$$L(w)-C\left(w,\sigma_x^r,\sigma_y^r,\tau_{xy}^r\right)=-\frac{\rho h}{D}\frac{\partial^2 w}{\partial t^2}-\frac{f_z}{D}, \tag{41}$$

$L(w)$ and $C(w,\sigma_x^r,\sigma_y^r,\tau_{xy}^r)$ in Eq. (41) are the same as those in Eq. (10). The distributed force f_z can be expressed in the same series as a displacement expression:

$$f_z=\sum_{m=1}^{M}\sum_{n=1}^{N}f_{mn}^z\sin(m\alpha x)\sin(n\beta y)\sin(\omega t). \tag{42}$$

Substituting Eqs. (11) and (42) into Eq. (41), and establishing the forced vibration of the stressed plate in the same way as above yields:

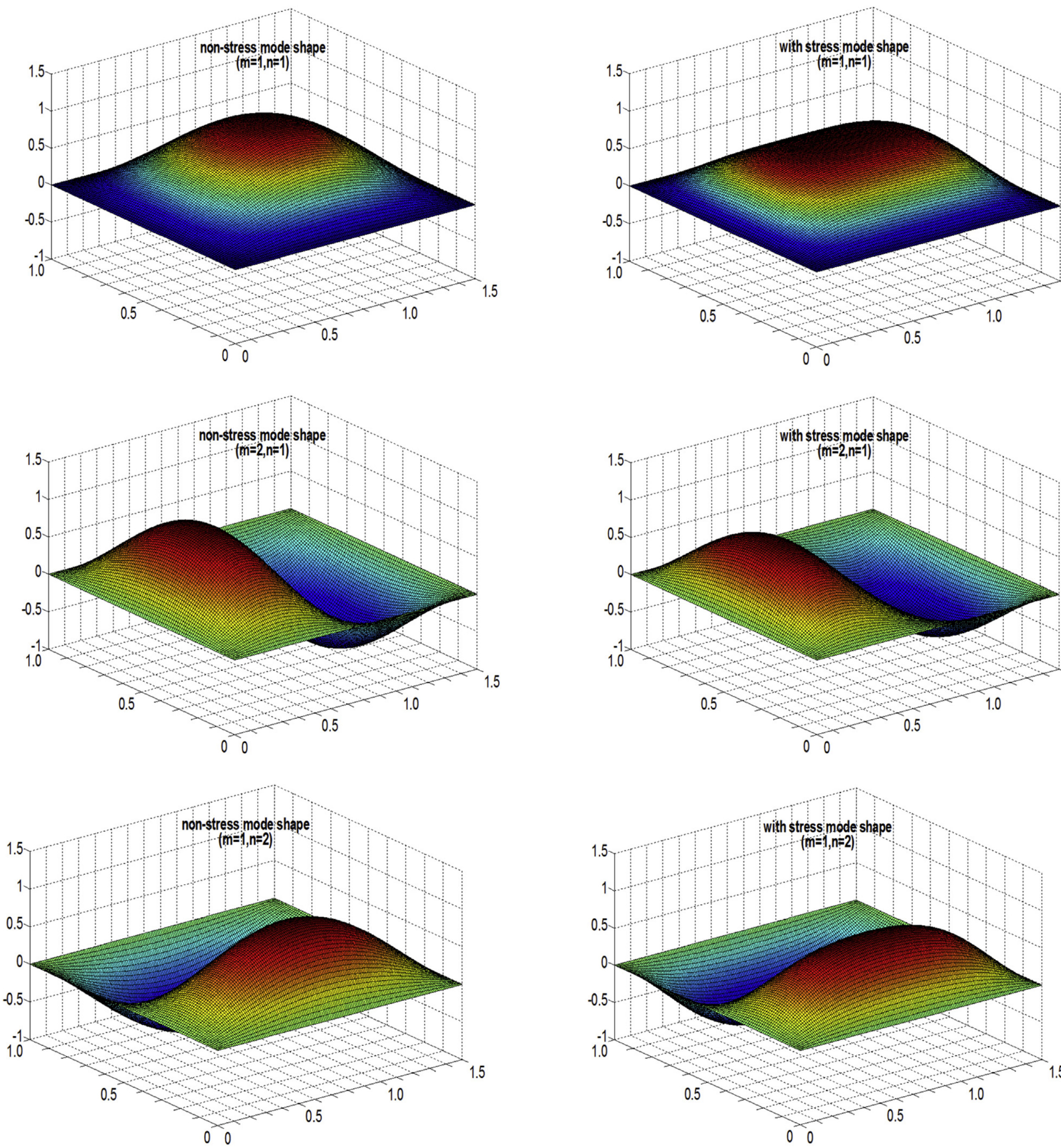

Fig. 8. The first 6 order mode shapes comparisons.

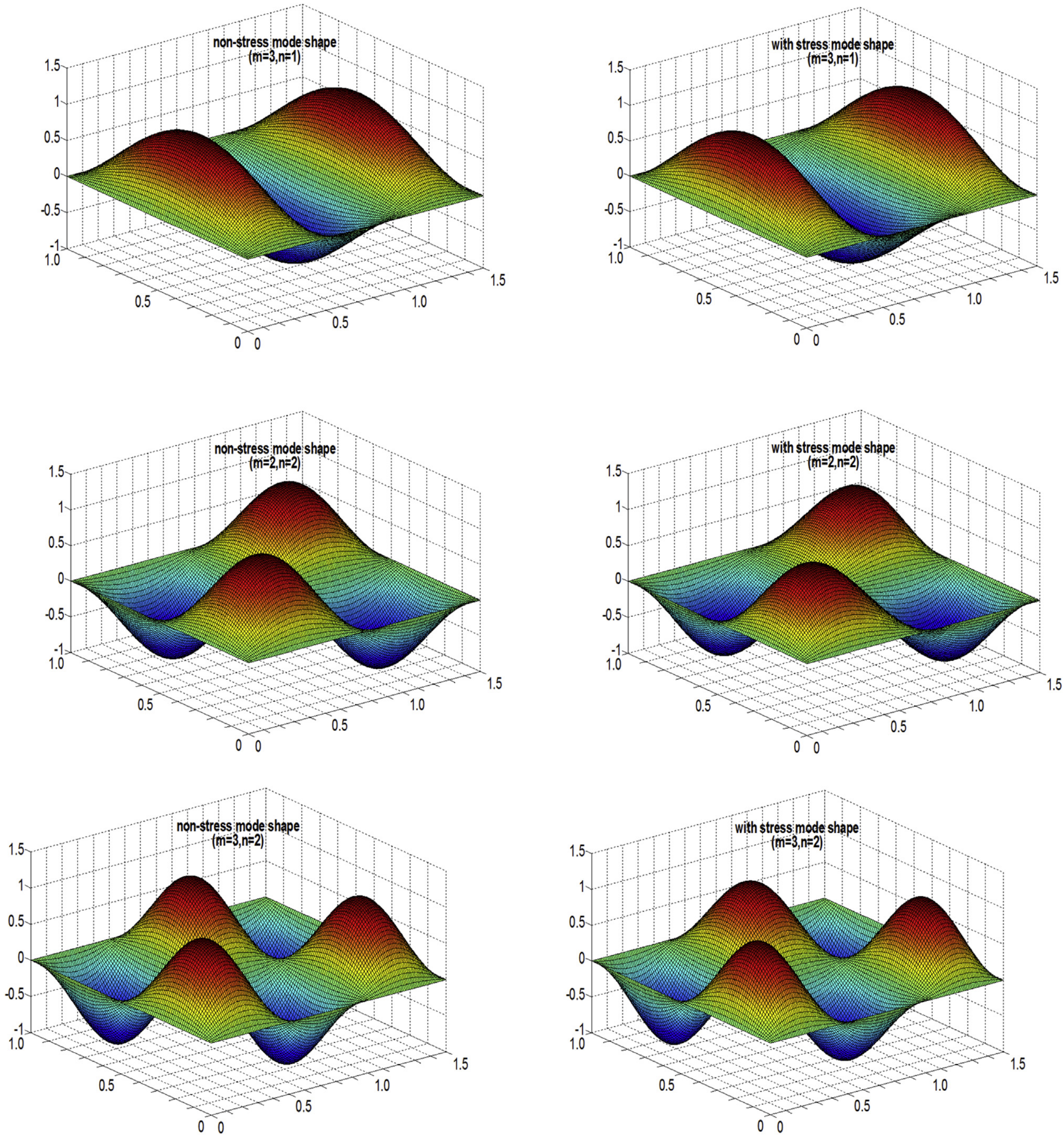

Fig. 8. (*continued*).

$$(\boldsymbol{\Lambda} + \boldsymbol{R})\boldsymbol{X} = \boldsymbol{F}. \tag{43}$$

The value of W_{mn} can be obtained by solving Eq. (43). Substitute these into Eq. (11) to obtain the forced vibration response of the plate with arbitrary stress distribution.

4. Numerical verification

In this section, the accuracy and advantage of the presented method is verified by using two numerical examples: one is a simple one-dimensional stress distribution case; the other is a practical stress distribution case.

4.1. One-dimensional stress example

A model of a stressed rectangular plate was created as shown in Fig. 6, and the colour represents the structural stress. The plate parameters are length $a = 1.5\ m$, width $b = 1\ m$, plate thickness $h = 0.01\ m$, density$\rho_s = 7860$ kg/m^3, Young's modulus $E = 2.1\ e^{11}\ N/m^2$, Poisson's ratio $\mu = 0.3$, and the boundary condition is simply supported. In this example, there exists only an x-directional stress, σ_x^r, in the plate, and the stress value varies only in the x direction. The stress distribution is shown in Fig. 7. The presented method is performed

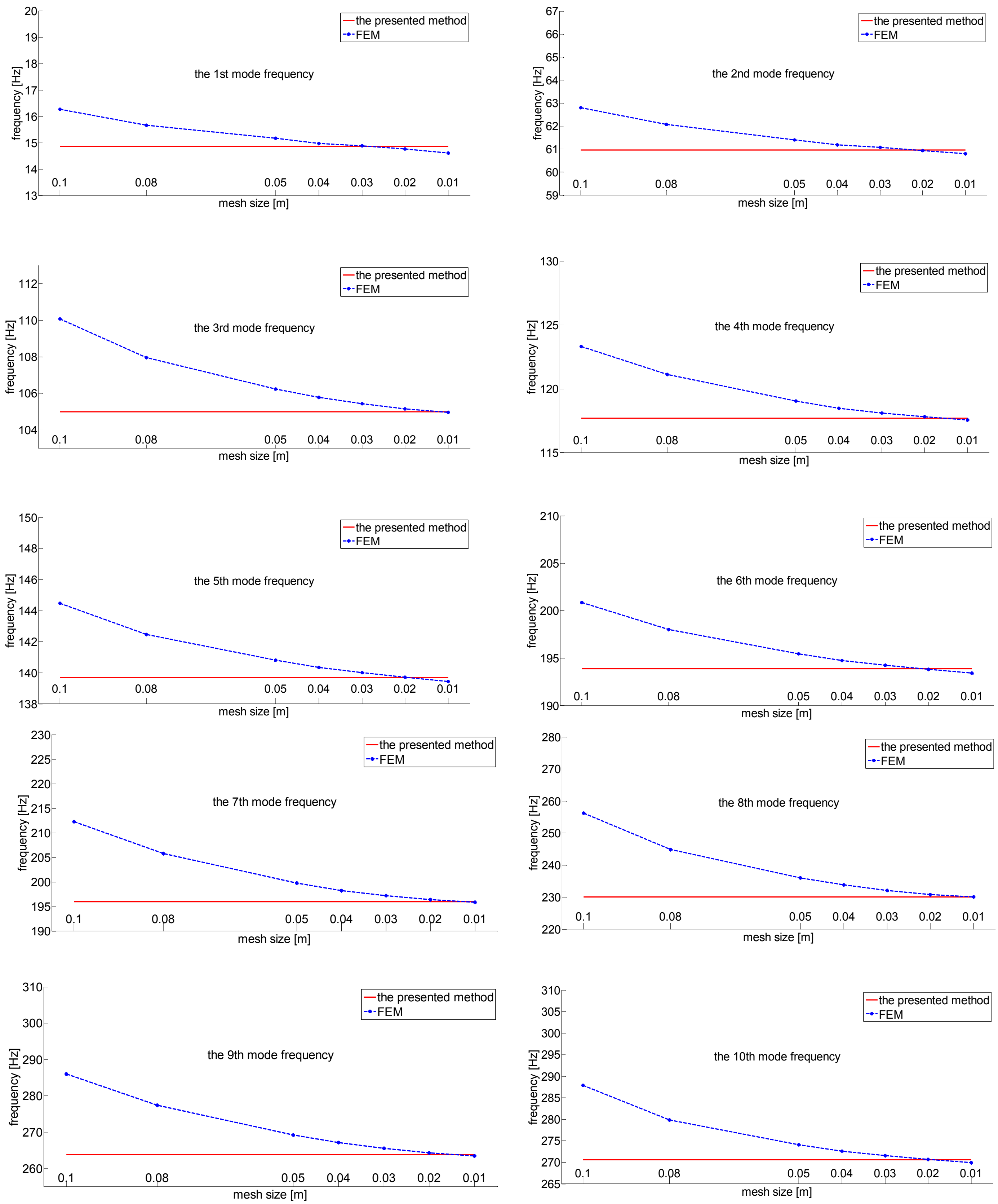

Fig. 9. Convergence analysis for the first 10 order modes.

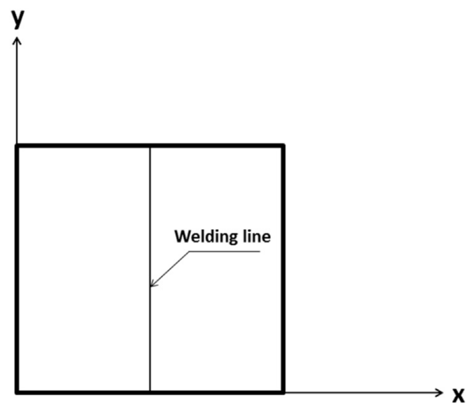

Fig. 10. Welding plate model.

by using Matlab R2013. The natural frequency and mode shapes of this model are calculated using the presented method and the FEM software Abaqus, respectively.

The mesh sizes (0.02, 0.03, 0.04, 0.05, 0.08, and 0.1 m) are selected in the FEM for comparison with the presented method. In Abaqus, the linear thin shell S4R5 element is selected as the element type. The number of series by the presented method is set to 100. The frequency results are listed in Table 1, the DOF comparison is listed in Table 2, and the mode shape results are shown in Fig. 8. The convergence analysis is shown in Fig. 9. The presented method is also applied in other boundary conditions. The results of different boundary conditions (including S−S−S−S, S−C−S−C, S−C−S−S and S−F−S−F) are listed in Table 3. In these cases, 0.02 m is selected as the FEM mesh size, the number of series by the presented method is 100. In order to avoid buckling, 0.8 Mpa is chosen as the stress amplitude for S−F−S−F, the other boundary conditions are all 100Mpa as seen in Fig. 7.

4.2. Practical stress example

In this section, a practical stress case, welding residual stress, is chosen as the numerical example. The welding stress distribution is more complicated than the stress in Section 4.1. The proposed method and the FEM are applied to calculate a welding plate's natural frequency, respectively. The welding plate is shown in Fig. 10. The plate model's geometric parameters are: length 2 m, width 2 m, and thickness 0.02 m, and its material properties are the same as in the previous example in Section 4.1. The welding line is located at $x = 1$ m.

The Thermo-Elastic-Plastic Finite Element Method (TEP-FEM) is used widely in welding simulation and welding residual stress calculations (Lee et al., 2013), and TEP-FEM software Marc was used to obtain the welding stress distribution in this plate. Based on the TEP-FEM welding residual stress results, the longitudinal and lateral welding residual stresses are fitted in series as shown in Fig. 11. Application of the presented method and Abaqus to solve the natural vibration of this welding plate yields the results in Table 4.

The results and convergence analysis show that as the mesh is refined, the results converge to a value that is close to the result obtained by using the presented method. And the presented method can also be applied in other boundary conditions. Therefore, the validity and accuracy of the presented method can be verified. Meanwhile, from Table 1 and Fig. 8, the stress changes the natural frequencies, but does not have an obvious influence on the mode shapes. In previous research, the influences of stress on the structure's ultimate strength and fatigue property have been paid more attention. However, according to the numerical examples, the effect of complex-distributed stress on structural dynamics also cannot be ignored.

Although for the pure computation time there does not appear to be much difference between the FEM and the presented method, the FEM requires many more complicated and time-consuming operations to exert a specified stress distribution during modelling. Moreover, when the mesh is updated or the stress distribution changes, these complicated operations have to be rerun. If the stress distribution changes frequently or the structure is very large and has a large number of elements, FEM modelling would be time-consuming.

Therefore, the presented method is more appropriate for studying the rule of the stress effects and for clarifying the essential relationship between structural stress and vibration. It has advantages for some qualitative research.

5. Conclusions

A unified solution for the vibration of plates with general structural stress distributions has been presented. The structural stress, regardless of its distribution and value, is expressed as a specific series, which can express almost all the

Table 3
Results of other boundary conditions.

Order	S−S−S−S		S−C−S−C		S−C−S−S		S−F−S−F	
	The method	FEM	The method	FEM	The method	FEM	The method	FEM
1	14.86	14.77	52.82	53.55	35.93	34.43	10.59	10.30
2	60.96	60.95	81.90	81.99	70.73	70.01	23.84	23.76
3	105.00	105.16	132.36	131.75	124.21	123.78	43.37	42.86
4	117.69	117.80	159.22	159.33	130.90	130.74	60.93	60.62
5	139.70	139.71	186.97	186.71	161.67	161.48	72.40	72.68
6	193.87	193.81	207.63	206.47	200.99	200.88	97.85	97.06

(Note: S-simply supported; C-clamped; F-free).

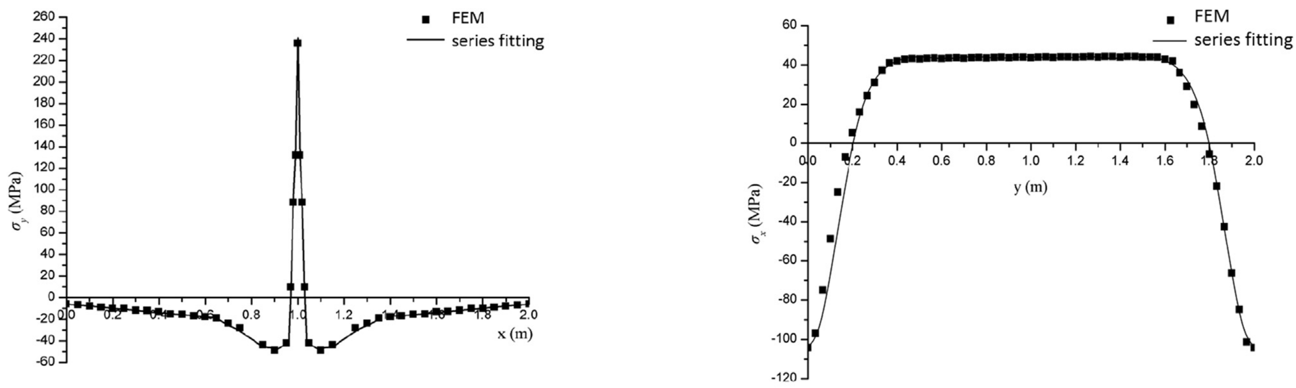

(a) longitudinal welding residual stress at y=1 (b) Lateral welding residual stress at x=1

Fig. 11. Plate welding residual stress.

Table 4
Results between presented method and FEM.

Order	(m, n)	Natural frequency (Hz)		
		Non-stress	With stress	
			Presented method	FEM
1	(1, 1)	24.39	28.64	29.11
2	(1, 2)	60.98	58.29	58.99
3	(2, 1)	60.98	64.08	64.75
4	(2, 2)	97.56	96.56	96.72
5	(1, 3)	121.95	123.28	124.10
6	(3, 1)	121.95	125.18	125.72
7	(2, 3)	158.54	158.38	158.63
8	(3, 2)	158.54	160.53	160.44
9	(1, 4)	207.32	208.41	207.61
10	(4, 1)	207.32	211.04	211.64

stress distributions and achieve partial decoupling among structural modes. The analytical solution obtained can be applied to a structure with arbitrary stress distributions, so it has a wider range of applications than the previous analytical methods. Meanwhile, it has the advantages of fewer modelling costs and provides a clearer physical explanation than the FEM, so that it is more convenient for researching the relationship between structural stress and vibration.

In this research, because of the impact on vibration, the distribution of structural stress is an important factor. Different stress distributions may have different impacts on structural vibration. The structural stress cannot be simplified into a uniform distributed stress in practical engineering structures, because this simplification may yield a large difference in the vibration results. In future, further study will be conducted on the effects of more practical stress distributions on the vibration characteristics by using the presented method to clarify the influential law between the vibration and non-uniform distributed stress.

Acknowledgements

The work presented in this paper was supported by the Fund of State Key Laboratory of Ocean Engineering (Grant No. 1507).

References

Ait Yahia, S., Ait Atmane, H., Houari, M.S.A., Tounsi, A., 2015. Wave propagation in functionally graded plates with porosities using various higher-order shear deformation plate theories. Struct. Eng. Mech. 53 (6), 1143–1165.

Belabed, Z., Houari, M.S.A., Tounsi, A., Mahmoud, S.R., Anwar Bég, O., 2014. An efficient and simple higher order shear and normal deformation theory for functionally graded material (FGM) plates. Compos. Part B 60, 274–283.

Bellifa, H., Benrahou, K.H., Hadji, L., Houari, M.S.A., Tounsi, A., 2016. Bending and free vibration analysis of functionally graded plates using a simple shear deformation theory and the concept the neutral surface position. J. Braz. Soc. Mech. Sci. Eng. 38, 265–275.

Bennoun, M., Houari, M.S.A., Tounsi, A., 2016. A novel five variable refined plate theory for vibration analysis of functionally graded sandwich plates. Mech. Adv. Mater. Struct. 23 (4), 423–431.

Bokaian, A., 2004. Thermal expansion of pipe-in-pipe systems. Mar. Struct. 17, 475–500.

Bouderba, B., Houari, M.S.A., Tounsi, A., 2013. Thermomechanical bending response of FGM thick plates resting on Winkler–Pasternak elastic foundations. Steel Compos. Struct. 14 (1), 85–104.

Bourada, M., Kaci, A., Houari, M.S.A., Tounsi, A., 2015. A new simple shear and normal deformations theory for functionally graded beams. Steel Compos. Struct. 18 (2), 409–423.

Brunelle, E.J., Robertson, S.R., 1976. Vibrations of an initially stressed thick plate. J. Sound Vib. 45 (3), 405–416.

Cao, Z., 1989. Vibration Theory of Plates and Shells. Chinese Railway Press.

Chen, L., Li, L., Zhang, Y., 2014. Characteristics analysis of structural-acoustic of cylindrical shell with prestress in local areas. J. Shanghai Jiao Tong Univ. 48 (8), 1084–1089.

Cho, D.S., Kim, B.H., Kim, J.H., Vladimir, N., Choi, T.M., 2016. Frequency response of rectangular plates with free-edge openings and carlings subjected to point excitation force and enforced displacement at boundaries. Int. J. Nav. Archit. Ocean Eng. 8 (2), 117–126.

Dong, P.A., 2001. Structural stress definition and numerical implementation for fatigue analysis of welded joints. Int. J. Fatigue 23 (10), 865–876.

Doong, J.L., 1987. Vibration and stability of an initially stressed thick plate according to a high-order deformation theory. J. Sound Vib. 113 (3), 425–440.

Fuller, C.R., Fahy, F.J., 1982. Characteristics of wave propagation and energy distributions in cylindrical elastic shells filled with fluid. J. Sound Vib. 81 (4), 501–518.

Gannon, L., Liu, Y., Pegg, N., et al., 2012. Effect of welding-induced residual stress and distortion on ship hull girder ultimate strength. Mar. Struct. 28 (1), 25–49.

Gao, Y., Su, Z., Jiao, Q., Tang, G., 2002. Influence on the natural frequency of component with residual stress. J. Mech. Strength 24 (2), 289−292.

Gao, Y., Tang, G., Wan, W., 2014. The calculations of natural frequency of quadrate thin plate with welding residual stress. J. Vib. Shock 33 (9), 165−167.

Hamidi, A., Houari, M.S.A., Mahmoud, S.R., Tounsi, A., 2015. A sinusoidal plate theory with 5-unknowns and stretching effect for thermomechanical bending of functionally graded sandwich plates. Steel Compos. Struct. 18 (1), 235−253.

He, Z., 2001. Structural Vibration and Radiation. Harbin Engineering University Press.

Hebali, H., Tounsi, A., Houari, M.S.A., Bessaim, A., Adda Bedia, E.A., 2014. A new quasi-3D hyperbolic shear deformation theory for the static and free vibration analysis of functionally graded plates. ASCE J. Eng. Mech. 140, 374−383.

Khan, I., Zhang, S., 2011. Effects of welding-induced residual stress on ultimate strength of plates and stiffened panels. Ships Offshore Struct. 6 (4), 297−309.

Lee, C.K., Chiew, S.P., et al., 2013. 3D residual stress modelling of welded high strength steel plate-to-plate joints. J. Constr. Steel Res. 84, 94−104.

Li, L., Wan, Z., Pan, G., Wang, Z., 2010. Review on welding residual stresses of submarine structures. Ship Sci. Technol. 32 (10), 130−134.

Liu, Z., 2009. Characteristics of Power Flow and Sound Radiation in Cylindrical Shell-fluid System Considering Hydrostatic Pressure. PhD Dissertation. Huazhong University of Science & Technology, Wuhan, China.

Liu, Z., Li, T., Zhu, X., et al., 2010. The effect of hydrostatic pressure fields on the dispersion characteristics of fluid-shell coupled system. J. Mar. Sci. Appl. 9 (2), 129−136.

Liu, Z., Li, T., Zhu, X., et al., 2011. The effect of hydrostatic pressure on input power flow in submerged ring-stiffened cylindrical shells. J. Ship Mech. 15 (3), 301−312.

Mahi, A., Adda Bedia, E.A., Tounsi, A., 2015. A new hyperbolic shear deformation theory for bending and free vibration analysis of isotropic, functionally graded, sandwich and laminated composite plates. Appl. Math. Model. 39, 2489−2508.

Meziane, Ait Amar, et al., 2014. An efficient and simple refined theory for buckling and free vibration of exponentially graded sandwich plates under various boundary conditions. J. Sandw. Struct. Mater. 16 (3), 293−318.

Niemi, E., 1995. Stress Determination for Fatigue Analysis of Welded Component. Woodhead Publishing.

Paik, J.K., Sohn, J.M., 2012. Effects of welding residual stresses on high tensile steel plate ultimate strength: nonlinear finite element method investigations. J. Offshore Mech. Arct. Eng. 134 (2), 021401.

Radaj, D., 2012. Heat Effects of Welding: Temperature Field, Residual Stress. Distortion. Springer Science & Business Media.

Senjanović, I., Vladimir, N., Cho, D.S., 2015. A new finite element formulation for vibration analysis of thick plates. Int. J. Nav. Archit. Ocean Eng. 7 (2), 324−345.

Senjanović, I., Vladimir, N., Tomić, M., 2016. On new first-order shear deformation plate theories. Mech. Res. Commun. 73, 31−38.

Tounsi, A., Houari, M.S.A., Benyoucef, S., Adda Bedia, E.A., 2013. A refined trigonometric shear deformation theory for thermoelastic bending of functionally graded sandwich plates. Aerosp. Sci. Technol. 24, 209−220.

Yahnioglu, N., 2007. On the stress distribution in a prestretched simply supported strip containing two neighboring circular holes under forced vibration. Int. Appl. Mech. 43 (10), 1179−1183.

Zhang, X.M., 2002. Frequency analysis of submerged cylindrical shells with the wave propagation approach. Int. J. Mech. Sci. 44 (7), 1259−1273.

Zhang, Y., Gorman, D., Reese, J., 2001a. A finite element method for modelling the vibration of initially tensioned thin-walled orthotropic cylindrical tubes conveying fluid. J. Sound Vib. 245 (1), 93−112.

Zhang, X.M., Liu, G.R., Lam, K.Y., 2001b. Coupled vibration analysis of fluid-filled cylindrical shells using the wave propagation approach. Appl. Acoust. 62 (3), 229−243.

Zidi, M., Tounsi, A., Houari, M.S.A., Adda Bedia, E.A., Anwar Bég, O., 2014. Bending analysis of FGM plates under hygro-thermo-mechanical loading using a four variable refined plate theory. Aerosp. Sci. Technol. 34, 24−34.